HHS Public Access

Author manuscript

Neuropeptides. Author manuscript; available in PMC 2021 August 01.

Published in final edited form as:

Neuropeptides. 2020 August ; 82: 102055. doi:10.1016/j.npep.2020.102055.

Impact of Caudal Hindbrain Glycogen Metabolism on A2 Noradrenergic Neuron AMPK Activation and Ventromedial Hypothalamic Nucleus Norepinephrine Activity and Glucoregulatory Neurotransmitter Marker Protein Expression

Ayed A. Alshamrani, **Khaggeswar Bheemanapally**, **Mostafa M.H. Ibrahim**, **Karen P. Briski**

School of Basic Pharmaceutical and Toxicological Sciences, College of Pharmacy, University of Louisiana Monroe, Monroe, LA 71201

Abstract

The brain glycogen reserve is a source of oxidizable substrate fuel. Lactoprivic-sensitive hindbrain A2 noradrenergic neurons provide crucial metabolic-sensory input to downstream hypothalamic glucose-regulatory structures. Current research examined whether hindbrain glycogen fuel supply impacts A2 energy stability and governance of ventromedial hypothalamic nucleus (VMN) metabolic transmitter signaling. Male rats were injected into the caudal fourth ventricle (CV4) with the glycogen phosphorylase inhibitor 1,4-dideoxy-1,4-imino-D-arabinitol (DAB) prior to continuous intra-CV4 infusion of L-lactate or vehicle. Lactate reversed DAB suppression of A2 neuron AMPK protein and up-regulated phosphoAMPK profiles. A2 dopamine-β-hydroxylase expression was refractory to DAB, but elevated by DAB/lactate. Lactate normalized A2 estrogen receptor-alpha and GPER proteins and up-regulated estrogen receptor-beta levels in DAB-treated rats. VMN norepinephrine content was decreased by DAB, but partially restored by lactate. DAB caused lactate-reversible or -irreversible augmentation of VMN glycogen phosphorylase-brain (GPbb) and -muscle type (GPmm) variant profiles, and correspondingly up- or down-regulated VMN protein markers of glucose-stimulatory nitrergic and glucose-inhibitory γ-aminobutyric acid

Correspondence: Dr. Karen P. Briski, Ph.D., Willis-Knighton Endowed Professor of Pharmacy, Director, School of Pharmaceutical and Toxicological Sciences, Professor of Pharmacology and Neuroanatomy, College of Pharmacy, University of Louisiana at Monroe, 356 Bienville Building, 1800 Bienville Drive, Monroe, LA 71201, TEL: 318-342-3283, FAX: 318-342-1737, briski@ulm.edu.

Author contributions:

Briski, Karen P.: Conceptualization, Resources, Supervision, Writing – Original Draft, Writing – Review & Editing, Project Administration, Funding Acquisition

Alshamrani, Ayed A.: Investigation, Formal analysis, Data curation, Visualization

Bheemanapally, Khaggeswar: Investigation, Formal analysis, Data curation, Visualization

Ibrahim, Mostafa M.H.: Investigation, Formal analysis, Data curation, Visualization

Statement on animal use: All animal experimental was carried out in compliance with the National Institutes of Health guide for the care and use of Laboratory animals (NIH Publications No. 8023, revised 1978), as stated in the submitted manuscript. Sex of animal used is included, along with discussion of impacts on study outcomes.

Declaration of interest: None.

Submission declaration and verification: The authors verify that this work has not been published previously, is not under consideration for publication elsewhere, that it is approved by all authors and tacitly by the University of Louisiana at Monroe, and that if accepted, it will not be published elsewhere in the same form with written consent of the copyright-holder.

transmission. DAB did not alter plasma glucose, but correspondingly suppressed or elevated circulating glucagon and corticosterone. Results show that diminished hindbrain glycogen breakdown is communicated to the VMN, in part by NE signaling, to up-regulate VMN glycogen breakdown and trigger neurochemical signaling of energy imbalance in that site. DAB effects on GPmm, VMN glycogen content, and counter-regulatory hormone secretion were unabated by lactate infusion, suggesting that aside from substrate fuel provision rate, additional indicators of glycogen metabolism such as glycogen mass may be monitored in the hindbrain.

Keywords

DAB; L-lactate; ventromedial hypothalamic nucleus; norepinephrine; 5'-AMP-activated protein kinase; neuronal nitric oxide synthase

Introduction:

Astrocytes promote neuro-metabolic stability through uptake, storage, and metabolism of glucose. Circulating glucose, the primary energy source to the brain, is taken up into these glia for either incorporation into the complex carbohydrate glycogen or conversion to the oxidizable substrate fuel L-lactate [Laming et al., 2000], which is transferred between astrocyte and neuron cell compartments by cell type-specific monocarboxylate transporters [Broer et al., 1997]. Lactate is a critical indicator of caudal hindbrain metabolic status [Patil and Briski, 2005]. Lactate repletion of that brainstem area normalizes hypothalamic metabolic transmitter expression during hypoglycemia, results that emphasize the physiological significance of hindbrain energy status for downstream glucose-regulatory function [Gujar et al., 2014]. Dorsal vagal complex (DVC) A2 noradrenergic neurons likely signal hypoglycemia-associated hindbrain substrate fuel imbalance as these cells exhibit lactate-reversible activation of the ultra-sensitive energy sensor adenosine 5'-monophosphate-activated protein kinase (AMPK], coincident with lactate-dependent augmentation of hypothalamic norepinephrine (NE) activity during hypoglycemia [Shrestha et al., 2014].

The hypothalamus integrates nutrient, endocrine, and neurochemical cues on metabolic status to shape motor outflow controlling glucose counter-regulation [Chan and Sherwin, 2014]. Dedicated metabolic-sensory neurons in the ventromedial hypothalamic nucleus (VMN) provide a dynamic cellular energy readout via increased ('fuel-inhibited'] or decreased ('fuel-excited'] synaptic firing in response to changes in substrate fuel provision [Oomura et al., 1969; Ashford et al., 1990; Silver and Erecinska, 1998]. Characterized effector transmitters of ventromedial hypothalamic energy insufficiency include nitric oxide (NO) and γ-aminobutyric acid (GABA), which correspondingly augment or suppress counter-regulatory hormone output [Chan et al., 2006; Fioramonti et al., 2011; Routh et al., 2014]. The likelihood of hindbrain noradrenergic control of these VMN neural signals is supported by evidence that biosynthetic enzyme protein markers of VMN glucose-regulatory signaling, e.g. neuronal nitric oxide synthase (nNOS) and glutamate decarboxylase$_{65/67}$ (GAD) are sensitive to exogenous NE [Ibrahim et al., 2019], and findings that both nerve cell populations express adrenergic receptor variant proteins [Uddin et al., 2019].

The astrocyte glycogen reservoir is dynamic during normal brain activity and metabolic stasis, and is a vital source of lactate equivalents during states of heightened function or glucose deficiency. The astrocyte glycogen shunt, which involves sequential glucose incorporation into and liberation from glycogen prior to entry into the glycolytic pathway, is an active process that accounts for a significant fraction of glucose catabolism in those cells. Current research investigated the hypothesis that glycogen breakdown is a critical screened variable in hindbrain monitoring of neuro-metabolic stability and regulation of hypothalamic metabolic transmission. Here, adult male rats were injected into the caudal fourth ventricle (CV4) with the glycogen phosphorylase (GP) inhibitor 1,4-dideoxy-1,4-imino-D-arabinitol (DAB) before continuous infusion of L-lactate or vehicle into the CV4. Pure A2 nerve cell samples were obtained by laser-catapult microdissection from sections cut through the caudal DVC for Western blot analysis of the metabolic-sensitive catecholamine biosynthetic enzyme dopamine-β-hydroxylase (DβH) and total and activated (phospho-) AMPK. In the female rat, A2 neurons express metabolic-sensitive estrogen receptor (ER] -alpha (ERα) and -beta (ERβ) proteins [Ibrahim and Briski, 2014], and these ERs may control hypoglycemic patterns of noradrenergic input to the reproductive neuroendocrine axis in that sex [Briski and Shrestha, 2016]. Present studies investigated whether A2 neurons in the male rat express one or both nuclear ER variants and/or the membrane estrogen receptor G protein-coupled estrogen receptor-1 (GPER) protein, and examined expressed ER proteins are sensitive to change in hindbrain glycogen breakdown. Additionally, VMN tissue was obtained by micropunch dissection for immunoblot analysis of glycogen metabolic enzyme, nNOS, and GAD protein profiles, NE measurement by ELISA, and UHPLC-electrospray ionization mass spectrometric (UHPLC-ESI-MS) analysis of tissue glycogen content.

Materials and Methods:

Animals:

Adult male Sprague Dawley rats (350-400 g bw) were housed under a 14 hr light/10 hr dark cycle (lights on at 05.00 hr), and allowed *ad-libitum* access to standard laboratory chow diet (Harlan Teklad LM-485;Harlan industries, Madison, WI) and tap water. All surgical and experimental protocols were conducted in accordance with NIH guidelines for care and use of laboratory animals, and approved by the ULM Institutional Animal Care and Use Committee. On Study day 1, animals were anesthetized with ketamine/xylazine (0.1 mL/100 g bw; 90 mg ketamine: 10 mg xylazine/mL; Henry Schein Inc., Melville, NY), and implanted with a 26-gauge stainless-steel cannula guide (prod no. C315G/SPC; Plastic One, Inc., Roanoke, VA) aimed at the caudal fourth ventricle (CV4) [coordinates: 13.3 mm posterior to bregma; 0 mm lateral to midline; 6.1 mm ventral to skull surface], by motorized computer-controlled stereotactic positioning (prod. no. 51700; Stoelting Co., Wood Dale,IL].

Experiment Design:

At 09.00 hr on day 7, animals were infused over a two minute period with the vehicle artificial cerebrospinal fluid (aCSF; 0.2 μL; group 1, n=7) or DAB (300 pM/0.2 μL [Boury-Jamot et al., 2016]; group 2 and 3, n=7 per group) into the CV4 using a 33-gauge 0.5 mm-projecting internal injection cannula (prod. no. C315I/SPC; Plastics One]. At 9.10 hr,

continuous infusion of aCSF (groups 1 and 2) or L-lactate (25 μM/2.0 μL/hr [Patil and Briski, 2005]; group 3), into the CV4 was initiated. At 10.00 hr, unanesthetized animals were sacrificed by microwave fixation (1.4 sec. exposure; In Vivo Microwave Fixation System, 5kW; Stoelting Co., Wood Dale, IL; n=4/group) or by decapitation (n=3 per each group) for brain tissue and trunk blood collection. Dissected brains were immediately frozen in liquid nitrogen-cooled isopentane for storage at −80°C. Plasma was stored at −20°C.

Western Blot Analysis of Laser-Catapult Microdissected DVC A2 Noradrenergic Nerve Cell Protein Expression:

Hindbrains obtained after decapitation were cut into serial 10 μm-thick frozen hindbrain sections between 14.36 to 14.86 mm posterior to *bregma*, and mounted on polyethylene naphthalate membrane slides (Carl Zeiss Microscopy LLC, Thornwood, NY). Tissues were fixed with acetone, blocked with 5% normal horse serum (Vectastain Elite ABC mouse IgG kit; Vector Laboratories, Inc., Burlingame, CA), then incubated for 24 hr at 4°C with a mouse monoclonal primary antiserum against tyrosine hydroxylase (TH; prod. no. 22941; 1:1,000; ImmunoStar, Inc., Hudson, WI). Sections were next treated sequentially with Vectastain IgG Elite ABC mouse IgG kit biotinylated secondary antibody, ABC reagent, and Vector DAB kit reagents (Vector Laboratories) to visualize TH-immunoreactive (-ir) neurons. Individual TH-ir cells exhibiting a visible nucleus and complete labeling of the cytoplasmic compartment were dissected using a Zeiss P.A.L.M. UV-A microlaser (Carl Zeiss Microscopy) and transferred to lysis buffer [2.0% sodium dodecyl sulfate, 0.05 M dithiothreitol, 10.0% glycerol, 1.0 mM EDTA, 60.0 mM Tris-HCl, pH 7.2]. For each protein of interest, A2 cell sample lysates from individuals subjects within a single treatment group were pooled (n=50 neurons/treatment group) ahead of separation on Bio-Rad TGX 10-12% stain-free gels (prod. no. 161-0183, Bio-Rad Laboratories Inc., Hercules CA) [Shakya et al., 2018]; each protein was analyzed in triplicate. Gels were UV light-activated (1 min.) in a Bio-Rad ChemiDoc TM Touch Imaging System prior to overnight protein transblotting (30 V, 4°C) to 0.45-μm PVDF membranes (ThermoFisherScientific; Waltham, MA). Membranes were pretreated with Western blotting signal enhancer (Pierce, Rockford, IL), then blocked with Tris-buffer saline (TBS), pH 7.4, containing 0.1% Tween-20 (Sigma Aldrich, St. Louis, MO) and 2% bovine serum albumin (MP Biomedicals, Solon, OH). Proteins of interest were probed using primary antisera raised in rabbit against $AMPK_{\alpha 1/2}$ (prod. no. 2532; 1:2,000; Cell Signaling Technology, Danvers, MA), phospho$AMPK_{\alpha 1/2}$-Thr 172 (pAMPK; prod. no. 2535; 1:2,000; Cell Signaling Technol.), DβH (prod. no sc-15318; 1:1,000; Santa Cruz Biotechnology, Inc., Santa Cruz, CA), ERβ/NR3A2 (prod. no. NB120-3577, 1:1,000; Novus Biologicals, LLC, Centennial, CO.) or GPER/GPR30 (prod. no. NLS 4271, 1:1,000; Novus Biol.), or in mouse against ERα/NR3A1 (prod. no. NB300560, 1:1,000; Novus Biol.). Membranes were incubated (1 hr) with horseradish peroxidase-labeled goat anti-rabbit (prod. no. NEF812001EA, 1:5,000; PerkinElmer, Waltham, MA) or goat anti-mouse (prod. no. NEF822001EA, 1:6000; PerkinElmer) secondary antibodies, then exposed to Supersignal West Femto maximum sensitivity chemiluminescent substrate (prod. no. 34096; ThermoFisherSci.). Membrane buffer washes and antibody incubations were performed by Freedom Rocker™ Blotbot® automation (Next Advance, Inc., Troy NY). Chemiluminescence band optical density (O.D.) values obtained in the ChemiDoc MP system were normalized to total in-lane protein with Imagelab software (Image Lab™ 6.0.0;

Bio-Rad). Precision plus protein molecular weight dual color standards (prod. no. 161-0374; Bio-Rad) were included in each Western blot analysis.

VMN Micropunch Dissection:

A repeating series of 100-150 μm-thick frozen sections were cut over the length of each microwave-fixed brain VMN in the following predetermined order: 1) 100 μm thickness, Western blotting; 2) 100 μm thickness, NE ELISA; 3) 150 μm thickness, LC-ESI-MS glycogen analysis; 4) 100 μm thickness, LC-ESI-MS lactate analysis. The VMN was identified relative to other forebrain structures using coronal rat brain section topographic features and neuroanatomical landmarks illustrated in rat brain atlases. VMN tissue was bilaterally removed from each tissue section using a calibrated 0.5 mm hollow punch tool (prod. no. 57401; Stoelting Co., Kiel, WI). Previous studies have verified the accuracy of micropunch methodology utilized in our laboratory for collection of distinctive hypothalamic loci of interest, including the VMN [Gujar et al., 2013; Alenazi et al., 2016; Mandal et al., 2017, 2018]. Micropunch samples used for immunoblotting were collected into lysis buffer, as described above; tissues utilized for ELISA were saved in lysis buffer made of 0.01 N HCl supplemented with 1.0 mM EDTA, 4.0 mM sodium metabisulfite; punches for LC-ESI-MS measurements were collected into 0.02 M Tris buffer, pH 7.2.

VMN Protein Western Blot Analysis:

For each protein of interest, tissue aliquots from individual subjects within a single treatment group were pooled in triplicate before Western blot analysis by BioRad Stain-Free technology, as described above. Proteins of interest were probed with polyclonal antisera raised in rabbit against glycogen synthase (GS; 1:2000; prod. no. 3893S; Cell Signaling Technology, Danvers, MA), glycogen phosphorylase-muscle type (GPmm; 1:2,000; prod. no NBP2-16689; Novus Biol.), glycogen phosphorylase-brain type (GPbb; 1:2,000; prod. no. NBP1-32799; Novus Biol.), nNOS (1:1,000; prod. no. Nbp1-396B1; Novus Biol.), or GAD (1:1,000; prod. no. ABN904; EMD Millipore, Billerica, MA).

VMN NE ELISA Analysis:

For each animal, micropunched VMN tissue was analyzed for NE content using Noradrenaline Research ELISA™ kit reagents (Labor Diagnostika Nord GmbH & Co KG, Nordhorn, Germany), as reported [Shrestha et al., 2014].

VMN Glycogen UHLC-ESI-MS Analysis:

Glycogen concentrations were determined in a ThermoFisherScientific Vanquish UHPLC+ System equipped with Thermo Scientific™ Dionex™ Chromeleon™ 7 Chromatography Data System software, as described [Bheemanapally et al., 2019]. Column and autosampler temperatures were 35°C and 15°C, respectively. The auto-sampler needle was washed with 10% (v/v) methanol (10 sec). Hydrolyzed and non-hydrolyzed samples were derivatized with 100 μL 0.5 M 1-phenyl-3-methyl-5-pyrazolone (PMP) reagent supplemented with 0.3 M NaOH. After acidification with 400 μL 0.75% formic acid, derivatized samples were extracted with chloroform to remove excess PMP, 400 μL of supernatant was vacuum concentrated to remove organic solvents, frozen at −80°C, and lyophilized. Lyophilization

product was diluted to 1.0 mL with 10 mM ammonium acetate, bath-sonicated (30 sec.), and centrifuged. Supernatant aliquots (250 μL) were transferred to 350 μL inserts, which were placed into 2 mL Surestop vials in an autosampler tray. D-(+)-Glucose-PMP was resolved using the Shodex™ Asahipak™ NH2P-40 3E column with a mobile phase (75:25 v/v), acetonitrile:10mM ammonium acetate (0.2 ml/min), D-(+]-Glucose-PMP ion chromatograms were extracted from Total Ion Current (TIC) at m/z 510.2 to generate area-under-the-curve data. Parameters for UHPLC-ESI-MS includes sheath gas pressure (SGP; 25 psig), auxiliary gas pressure (AGP; 4.6 psig), sweep gas pressure (SWGP; 0.5 psig), vaporizer temperature (VT; 150°C), ion transfer tube temperature (ITT; 150°C), source voltage (−2000V), foreline pressure (1.76 Torr; auto-set by instrument- and variable), source gas (nitrogen; Genius NM32LA 110V, 10-6520; Peak Scientific, Inchinnan, Scotland), and mass peak area detection algorithm (ICIS/Genesis) were maintained at optimum.

Glucose and Counter-Regulatory Hormone Measurements:

Plasma glucose levels were determined using an ACCU-CHECK Aviva plus glucometer (Roche Diagnostic Corporation, Indianapolis, IN) [Kale et al., 2006). Plasma corticosterone (ADI-900-097; Enzo Life Sciences, Inc., Farmingdale, NY) and glucagon (EZGLU-30K, EMD Millipore, Billerica, MA) concentrations were determined using commercial ELISA kit reagents [Alhamani et al., 2018].

Statistical analyses:

Mean normalized Western blot protein O.D., VMN tissue NE, VMN tissue glycogen, and plasma glucose, glucagon, and corticosterone data were evaluated between treatment groups by one-way analysis of variance and Student Newman Keuls *post-hoc* test. Differences of $p < 0.05$ were considered significant.

Results:

Figure 1 depicts combinatory immunocytochemical labeling and laser-catapult microdissection of individual TH-immunopositive hindbrain dorsal vagal complex A2 neurons for Western blot analyses. Individual nerve cells in hindbrain tissue sections were identified by TH-ir prior to laser-catapult harvesting [Panel A]; representative stained neurons are indicated by blue arrows. Middle and right-hand columns illustrate actions, including sequential positioning of continuous laser cuts (shown in green in Panel B) surrounding separate distinctive neurons, that result in removal of single cells without destruction of surrounding tissue and minimal inclusion of adjacent tissue (Panel C).

Figure 2 depicts effects of intra-CV4 administration of the GP inhibitor DAB with our without subsequent L-lactate infusion on DVC A2 nerve cell total AMPK and pAMPK, DβH, and ER variant protein expression. Data in Panel 2A show that DAB significantly reduced A2 AMPK profiles [$F_{(2,6)}$) = 8.49, $p = 0.003$], but that ensuing lactate repletion prevented this inhibitory response. A2 pAMPK expression was not affected by DAB treatment, but was greater in DAB/lactate versus DAB/V and V/V groups (Panel 2B) [$F_{(2,6)}$ = 6.65, $p = 0.01$]. As illustrated in Panel 2C, A2 DβH protein expression was refractory to DAB, but was significantly augmented in response to combinatory DAB plus lactate

treatment compared to DAB/V or V/V treatment [$F_{(2,6)} = 7.19$, $p = 0.009$]. Inhibitory effects of DAB on A2 ERα (Panel 2D) [$F_{(2,6)} = 9.19$, $p = 0.002$] and GPER (Panel 2F) [$F_{(2,6)} = 11.22$, $p = 0.004$] protein profiles were reversed by lactate. DAB did not elicit measureable change in A2 ERβ content (Panel 2E), but this profile was up-regulated in DAB/lactate versus DAB/V and V/V treatment groups [$F_{(2,6)} = 7.37$, $p = 0.006$].

Data in Figure 3 portray effects of hindbrain L-lactate repletion on DAB regulation of VMN NE activity. DAB administration significantly reduced tissue NE content, but catecholamine levels were partially normalized by subsequent lactate infusion [$F_{(2,9)} = 208.00$, $p < 0.0001$]. VMN glycogen metabolic enzyme and glucose-stimulatory and -inhibitory neurotransmitter marker protein responses to DAB, in the presence versus absence of L-lactate infusion, are presented in Figure 4. As shown in Panel 4A, VMN GS protein expression was refractory to DAB plus V or lactate administration [$F_{(2,6)} = 0.31$, $p = 0.733$]. VMN GPmm content was significantly increased by DAB, but this stimulatory response was unaffected by exogenous lactate (Panel 4B) [$F_{(2,6)} = 10.73$, $p = 0.004$]. While DAB also up-regulated VMN GPbb protein expression, drug-induced augmentation of this profile was prevented by CV4 lactate infusion (Panel 4C) [$F_{(2,6)} = 6.92$, $p = 0.015$]. Data in Panel 4D show that DAB significant reduced VMN tissue glycogen levels, and that this response was refractory to hindbrain lactate infusion [$F_{(2,9)} = 9.49$, $p = 0.0002$]. Diminution of VMN tissue glucose content by DAB was reversed by lactate (Panel43E) [$F_{(2,9)} = 38.16$, $p < 0.0001$].

Results shown in Figure 5 depict effects of DAB with or without hindbrain lactate repletion on VMN nNOS or GAD protein expression. As shown in Panel 5A, DAB up-regulation of nNOS profiles was normalized by lactate infusion [$F_{(2,6)} = 4.16$, $p = 0.019$]. VMN GAD protein was suppressed by DAB (Panel 5B), a response that was partially reversed by lactate [$F_{(2,6)} = 21.56$, $p = 0.0001$].

As indicated in Figure 6, panel A, intra-CV4 DAB administration did not alter plasma glucose concentrations, irrespective of subsequent infusate [$F_{(2,19)} = 0.04$, $p = 0.96$]. Data in Panel 6B indicate that DAB suppressed circulating glucagon levels, but that this drug effect was not modified by lactate [$F_{(2,19)} = 4.11$, $p = 0.02$]. Plasma corticosterone concentrations were significantly elevated in response to DAB (Panel 6C), but secretion was equivalent between DAB/lactate versus DAB/V treatment groups [$F_{(2,19)} = 5.16$, $p = 0.02$].

Discussion:

The present project examined the premise that hindbrain metabolic sensors monitor local glycogen turnover/depletion and impart hindbrain glycogen metabolic status to the brain glucostatic network. Results show that reduced hindbrain glycogen disassembly and consequent diminution of lactate provision enhance metabolic-sensitive A2 noradrenergic neuron AMPK activity. A2 DβH protein and VMN NE content were respectively unchanged or suppressed by DAB, but were both up-regulated by combinatory DAB/lactate treatment. These data suggest that NE input to the VMN is sensitive to hindbrain glycogen status, and that the ratio of A2 NE synthesis/VMN NE release may be increased by dwindled hindbrain glycogen mobilization and normalized by exogenous lactate repletion. Lactate-reversible inhibition of A2 neuron ERα and GPER protein expression by DAB implies that glycogen-

derived fuel decrements alter A2 nerve cell reactivity to estradiol; further work is needed to determine if adapted estradiol signaling is a cause or, alternatively, an outcome of A2 detection of decreased metabolic fuel provision. Major findings of current research include novel proof that decreased hindbrain glycogen mobilization enhances VMN glycogen breakdown and augments VMN transmitter signals of energy deficiency. Evidence here that hindbrain lactate repletion did not prevent DAB effects on VMN GPmm protein expression, VMN glycogen content, or counter-regulatory hormone secretion, infers that additional known indicators of hindbrain glycogen metabolism, aside from glycogen-derived energy fuel volume such as glycogen mass, may be communicated to downstream hypothalamic glucoregulatory loci.

Data show that DAB suppresses A2 neuron AMPK protein content, but does not alter pAMPK expression, suggesting that diminution of hindbrain glycogen mobilization may increase enzyme specific activity. Normalization of total AMPK levels by lactate infusion infers that total protein production is sensitive to disruption of glycogen-derived substrate fuel provision. Current outcomes align with studies showing that hindbrain monocarboxylate transporter inhibition by alpha-cyano-4-hydroxycinnamic acid (4CIN) down-regulates A2 AMPK expression and increases the cellular pAMPK/AMPK ratio [Briski and Mandal, 2019]. Discrepant effects of DAB versus 4CIN on A2 pAMPK profiles may reflect, in part, differences in degree or magnitude of decline in endogenous lactate trafficking owing to respective drug targeting of lactate derived from glycogen versus total lactate available for membrane transport. Present outcomes do not clarify the molecular mechanisms that underlie treatment effects on total AMPK content; however, it can be speculated that this protein profile may be sensitive to altered plasma membrane and/or mitochondrial monocarboxylate transporter activity. The lack of DAB effect on A2 pAMPK expression suggests that energy imbalance is maintained despite lactate deficiency, suggesting that these cells may rely, over an undetermined time frame, on alternative oxidizable energy substrates such as glucose or glucogenic amino acids. Interestingly, exogenous lactate infusion up-regulated A2 pAMPK expression while normalizing total A2 AMPK levels; results thus depict augmented proportionate activation of AMPK by either DAB alone or DAB plus lactate treatment, albeit by corresponding down-regulation of total AMPK versus up-regulation of pAMPK. Data here infer that A2 AMPK expression may be sensitive to decreased metabolic fuel supply, whereas pAMPK augmentation despite regularization of AMPK may signal reductions in glycogen turnover or shunt activity alongside no net disruption of astrocyte exportation of oxidizable substrate fuel. It is possible that communication between astrocytes and neurons regarding astrocyte energy reserve size and turnover is not limited to volume of trafficked lactate, but may also involve neurochemical signals that regulate nerve cell energy stability.

Our working premise was that A2 DβH protein responses to CV4 DAB administration would parallel demonstrable drug effects on A2 AMPK activity, yet current data show that DβH profiles were refractory to DAB. It is noted that measures of enzyme protein are not a definitive indicator of enzyme activity; thus, it is possible that DAB may impact the function of DβH and/or other enzymes in the A2 nerve cell catecholamine biosynthetic pathway, and thus modify NE synthesis, without affecting their expression profiles. This supposition is bolstered by observations here that VMN NE content declines after DAB treatment, and that

exogenous lactate attenuates this inhibitory response as well as up-regulates A2 DβH expression. Aside from documenting sensitivity of VMN NE activity to hindbrain glycogen metabolism, present data imply that the ratio of A2 NE synthesis/VMN NE release is amplified by dwindled hindbrain glycogen mobilization and regularized by substrate fuel repletion. It is useful to point out that diminished hindbrain glycogen fuel supply is apparently communicated to the VMN by a reduction in NE input. The direction of this NE response differs from that elicited by insulin-induced hypoglycemia where VMN NE levels are increased alongside augmented A2 nerve cell DβH protein expression [Mandal and Briski, 2018]. These outcomes support the notion that A2 neurons may be able to signal varying intensities or nature of metabolic imbalance in part by reducing or amplifying NE signal strength. Indeed, electro-physiological mapping of the DVC showed that 'glucose-excited (GE)' and 'glucose-inhibited (GI)' neurons reside primarily in the A2 area [Mizuno and Oomura, 1984], where both of these phenotypes were ascribed to catecholaminergic neurons [Yettefti et al., 1997]. The current presumption that CV4 DAB versus peripheral insulin injection treatment paradigms likely have dissimilar effects on volume of lactate trafficked to A2 neurons remains speculative due to a lack of technological capability for quantification of magnitude of change in trafficked lactate occurring under each experimental condition. Nevertheless, it could be contended that DAB would likely have a relatively lesser disruptive impact on substrate fuel stream as only lactate yield from the glycogen reserve (not from glucose bypassing the glycogen shunt) would supposedly be reduced by that drug treatment, whereas effects of hypoglycemia are apt to be more profound as this systemic condition diminishes net amount of glucose taken up by astrocytes and available for lactate metabolism. Along the same lines, it would be of interest to determine if up-regulated DβH due to DAB plus lactate treatment drives GI signaling of suppressed glycogen turnover/shunt activity or depletion, or alternatively, reflects attenuation of DAB inhibition of GE signaling. It remains to be determined if distinct subsets of A2 nerve cells function exclusively as GE or GI, or if individual A2 cells are capable of bi-directional signaling depending upon extent/type of metabolic imbalance.

The present project sought to investigate hindbrain glycogen metabolism effects on A2 ER variant protein expression as prior work showed that distinct metabolic stressors such as short-term food deprivation [Briski et al., 2014] and insulin-induced hypoglycemia (IIH) [Shrestha et al., 2015] affect dorsal vagal complex or A2 cell sample ER protein profiles, respectively, in female rats, and that ER-beta may mediate unanticipated IIH up-regulation of A2 noradrenergic signaling during estrogen positive-feedback activation of the reproductive neuroendocrine axis in that sex [Briski and Shrestha, 2016]. Current evidence for DAB-induced down-regulation of A2 neuron ERα and GPER proteins shows that decrements in glycogen-derived energy fuel affect cellular reactivity to estradiol in this sex. It would be insightful to learn if and how adjusted signaling by these individual ER variants may impact cellular function, including metabolic sensory signaling. Moreover, it would be informative to learn if ERα and/or GPER mediate DAB effects on AMPK activity and NE synthesis, or conversely, receptor numbers are adjusted in response to sensor detection of metabolic imbalance. Data here also show that A2 cells exhibited parallel amplification of pAMPK, DβH, and ERβ protein profiles in response to combinatory DAB/lactate treatment. Current studies do not shed light on whether enhanced ERβ input to A2 neurons is a cause

versus consequence of enhanced AMPK phosphorylation and/or DβH expression. Present findings provide a justifiable foundation for ongoing studies that seek to determine if metabolic-sensitive ERs act directly on A2 neurons to shape transmitter function during exposure to different metabolic stress conditions.

Present outcomes provide unique evidence that hindbrain glycogen metabolic status governs VMN glycogen breakdown and gluco-regulatory transmitter signaling. GP activity is controlled by serine phosphorylation and/or stimulatory (AMP) and inhibitory (glucose) allosteric effectors [Griffiths et al., 1976; Barford and Johnson, 1989]. In the brain, GPmm and GPbb show differential sensitivity to phosphorylation and AMP regulation [Nadeau et al., 2018]. Phosphorylation fully activates GPmm, but not GPbb, which requires AMP binding for maximum activation [Mathieu et al., 2016]. AMP exhibits greater binding affinity for GPbb versus GPmm, and reduces GPbb Km for glycogen [Lowry et al., 1967]. In brain, GPmm mediates noradrenergic stimulation of cortical astrocyte glycogenolysis *in vitro*, whereas GPbb mobilizes glycogen breakdown during energy deficiency [Müller et al., 2015]. Current results show that intra-CV4 DAB administration up-regulated VMN GPbb and GPmm protein profiles. Although changes in total GPbb and GPmm protein expression do not constitute definitive proof of commensurate changes in enzyme activity, UPLC-ESI-MS documentation of DAB-induced reductions in VMN glycogen content is consistent with increased VMN GP enzyme activity. As data here show that DAB suppresses VMN NE activity, the extent to which local GPmm activity may be affected by decrements in this regulatory input is unclear. Exogenous lactate infusion prevented DAB enhancement of VMN GPbb, but not GPmm profiles; these data indicate that the former, but not latter GP variant is response to drug effects on glycogen-derived fuel supply and that VMN GPmm expression is sensitive to an alternative cue(s) of hindbrain glycogen metabolic state, possibly information on rate of glycogen turnover or disassembly *per se* or, alternatively, relative to glycogen mass. Lactate was ineffectual in preventing DAB-mediated VMN glycogen breakdown, suggesting that this drug effect may be primarily mediated by GPmm. Surprisingly, DAB treatment elicited reductions in net VMN tissue glucose content. This response may reflect either a decline in glucose uptake from the circulation directly into neural tissue extracellular space, or alternatively, increased glucose utilization in energy- and non-energy pathways. Further research is needed to investigate effects of hindbrain DAB administration on VMN endothelial cell and neuron glucose transporter expression and function.

Hindbrain DAB administration caused lactate-reversible up- or down-regulation of marker proteins for VMN transmitters that stimulate (NO) or inhibit (GABA) counter-regulation. As drug-treated animals exhibited these signals of energy deficiency alongside increased VMN glycogen breakdown, it is plausible that NO and GABA neurons may be direct targets for hindbrain stimuli that inform on hindbrain glycogen metabolic status, and that reactivity of these nerve cells to such cues may be mitigated, to some extent, by DAB-associated VMN glycogen mobilization and/or changes in VMN glucose provision/utilization. We theorize that one or both glucoregulatory cell populations may receive direct noradrenergic input as both types express multiple adrenergic receptor variants proteins [Uddin et al., 2019]; however, this premise will require experimental validation.

Current data show that DAB treatment did not modify plasma glucose concentrations, yet had significant effects on counter-regulatory hormone secretion. Accordingly, signals of glycogen metabolic dysfunction that originate within a relatively small volume of brain tissue may be ineffectual in terms of producing a net significant change in glycemic profiles. Observations here of converse regulatory effects of DAB on plasma glucagon and corticosterone levels may reflect an overall negligible impact of counter-regulatory hormones on plasma glucose. DAB augmentation of corticosterone release is consistent with induction of hyperocorticosteronemia by hindbrain delivery of the monocarboxylate transporter inhibitor alpha-cyano-4-hydroxycinnamic acid (4CIN) [Briski and Mandal, 2019; personal communication]. Yet, whereas 4CIN stimulated glucagon secretion, DAB inhibited this hormone profile here. It is speculated that glucagon decrements due to DAB may be causally related, in part, to augmentation of circulating free fatty acid levels as that substrate fuel is reported to inhibit glucagon secretion [Gerich et al., 1974; Luyckx et al., 1978].

In summary, the present project examined whether hindbrain metabolic sensor detection of glycogen turnover/depletion governs hypothalamic glucose-regulatory transmitter function. Main results include evidence that suppression of hindbrain glycogen disassembly causes lactate-revocable changes in metabolic-sensory A2 noradrenergic neuron AMPK activity and VMN NE content. Lactate-reversible inhibitory impact of DAB on A2 ERα and GPER protein profiles infers that glycogen-derived energy fuel supply alters estradiol signaling to these neurons. DAB-mediated up- or down-regulation of VMN glucose-stimulatory nitrergic and -inhibitory GABAergic signaling was averted by lactate, which demonstrates sensitivity of critical hypothalamic glucoregulatory transmitters to hindbrain glycogen metabolism. Evidence that VMN GPmm, VMN glycogen, and glucagon and corticosterone responses to DAB were refractory to exogenous lactate implies that additional indicators of glycogen metabolism, aside from screened glycogen-derived energy fuel stream, may be communicated from the hindbrain to the VMN gluco-regulatory circuitry.

Acknowledgments

Funding source: This research was funded by National Institutes of Health grant DK 109382.

Abbreviations:

CV4	caudal fourth ventricle
DAB	1,4-dideoxy-1,4-imino-d-arabinitol
DβH	dopamine-beta-hydroxylase
DVC	dorsal vagal complex
ERα	estrogen receptor-alpha
ERβ	estrogen receptor-beta
GABA	γ-aminobutyric acid
$GAD_{65/67}$	glutamate $decarboxylase_{65/67}$

GP_{mm}	glycogen phosphorylase-muscle type
GP_{bb}	glycogen phosphorylase-brain type
GPER	G protein-coupled estrogen receptor 1
GS	glycogen synthase
NE	norepinephrine
NO	nitric oxide
nNOS	neuronal nitric oxide synthase
VMN	ventromedial hypothalamic nucleus

References:

Alenazi FSH, Ibrahim BA, AlHamami H, ShakYa M, Briski KP. Role of estradiol in intrinsic hindbrain AMPK regulation of hypothalamic AMPK, metabolic neuropeptide, and norepinephrine activity and food intake in the female rat. Neuroscience 2016; 314: 35–46. [PubMed: 26628404]

Alhamami HN, Alshamrani A, Briski KP, 2018 Effects of the glycogen phosphorylase inhibitor 1,4-dideoxy-1,4-imino-D-arabinitol on ventromedial hypothalamic nucleus 5'-adenosine monophosphate-activated protein kinase activity and metabolic neurotransmitter biosynthetic enzyme protein expression in eu- versus hypoglycemic male rats. Physiol. Report 103, 236–249.

Ashford MLJ, Boden PR, Treherne JM. Glucose-induced excitation of hypothalamic neurons is mediated by ATP-sensitive K+ channels. Pfugers Arch. 1990; 415: 479–483.

Barford D, Johnson LN. The allosteric inhibition of glycogen phosphorylase. Nature 1989; 340: 8381–8389.

Boury-Jamot B, Carrard A, Martin JL, Halfon O, Magistretti PJ, Boutrel B Disrupting astrocyte-neuron lactate transfer persistently reduced conditioned responses to cocaine. Mol. Psych 2016; 21: 1070–1076.

Briski KP, Mandal SK. Hindbrain lactoprivic regulation of hypothalamic neuron transactivation and glucoregulatory neurotransmitter expression: Impact of antecedent insulin-induced hypoglycemia. Neuropeptides 2019; doi: 10.1016/j.npep.2019.101962.

Briski KP, Ibrahim BA, Tamrakar P. Energy metabolism and hindbrain AMPK: regulation by estradiol. Horm. Mol. Biol. Clin. Invest 2014; 17: 129–136.

Briski KP, Shrestha PK. Hindbrain estrogen receptor-beta antagonism normalizes reproductive and counter-regulatory hormone secretion in hypoglycemic steroid-primed ovariectomized female rats. Neuroscience 2016; 331:62–71. [PubMed: 27316550]

Broer S, Rahman B, Pellegri G, Pellerin L, Martin JL, Verleysdonk S, Hamprecht B, Magistretti PJ. Comparison of lactate transport in astroglial cells and monocarboxylate transporter (MCT 1) expressing Xenopus laevis oocytes. Expression of two different monocarboxylate transporters in astroglial cells and neurons. J. Biol. Chem 1997; 272: 30096–30102. [PubMed: 9374487]

Chan O, Sherwin R Influence of VMN fuel sensing on hypoglycemic responses. Trends Endocrinol. Metab. 2013; 24, 616–624. [PubMed: 24063974]

Chan O, Zhu W, Ding Y, McCrimmon RJ, Sherwin RS. Blockade of GABA(A) receptors in the ventromedial hypothalamus further stimulates glucagon and sympathoadrenal but not the hypothalamo-pituitary-adrenal response to hypoglycemia. Diabetes 2006; 55: 1080–1087. [PubMed: 16567532]

Gerich JE, Langlois M, Schneider V, Karam JH, Noacco C. Effects of alterations of plasma free ratty acid levels on pancreatic glucagon secretion in man. J. Clin. Invest 1974; 53: 1284–1289. [PubMed: 4825225]

Fioramonti X, Song Z, Vazirani RP, Beuve A, Routh VH. Hypothalamic nitric oxide in hypoglycemia detection and counterregulation: a two-edged sword. Antioxid. Redox Signal 2011; 14: 505–517 [PubMed: 20518706]

Griffiths JR, Dwek RA, Radda GK. Heterotropic interactions of ligands with phosphorylase B. Eur. J. Biochem 1976; 61: 234–251.

Gujar AD, Ibrahim BA, Tamrakar P, Briski KP. Hypoglycemia differentially regulates hypothalamic glucoregulatory neurotransmitter gene and protein expression: Role of caudal dorsomedial hindbrain catecholaminergic input. Neuropeptides 2013; 47: 139–147. [PubMed: 23490004]

Gujar AD, Ibrahim BA, Tamrakar P, Koshy Cherian A, Briski KP. Hindbrain lactostasis regulates hypothalamic AMPK activity and hypothalamic metabolic neurotransmitter mRNA and protein responses to hypoglycemia. Amer. J. Physiol. Regul. Integr. Comp. Physiol 2014; 306: R457–R469. [PubMed: 24381179]

Ibrahim MMH, Alhamami HN, Briski KP. Norepinephrine regulation of ventromedial hypothalamic nucleus metabolic transmitter biomarker and astrocyte enzyme and receptor expression: role of 5'-AMP-activated protein kinase. Brain Research 2019; 1711: 48–57. [PubMed: 30629946]

Kale AY, Paranjape SA, Briski KP. I.c.v. administration of the nonsteroidal glucocorticoid receptor antagonist, CP4-72555, prevents exacerbated hypoglycemia during repeated insulin administration. Neuroscience 2006; 140: 555–565. [PubMed: 16626867]

Laming PR, Kimelberg H, Robinson S, Salm A, Hawrylak N, Muller C, Roots B, and Ng K. Neuronal-glial interactions and behavior. Neurosci. Biobehav. Rev 2000; 24: 295–340. [PubMed: 10781693]

Lowry OH, Schulz DW, Passonneau JV. The kinetics of glycogen phosphorylases from brain and muscle. J. Biol. Chem 1967; 2142: 271–280.

Luyckx AS, Gaspard U, Lefebvre PJ. Influence of elevated plasma free fatty acids on the glucagon response to hypoglycemia in normal and in pregnant women. Metabolism 1978; 27: 1033–1040. [PubMed: 682968]

Mandal SK, Briski KP. Hindbrain dorsal vagal complex AMPK controls hypothalamic AMPK activation and metabolic neurotransmitter protein expression and counter-regulatory hormone secretion in the hypoglycemic male rat. Brain Res. Bull 2018; 144:171–179. [PubMed: 30481553]

Mandal SK, Shrestha PK, Alenazi FSH, Shakya M, Alhamami HN, Briski KP. Role of hindbrain adenosine 5'-monophosphate-activated protein kinase (AMPK) in hypothalamic AMPK and metabolic neuropeptide adaptation to recurring insulin-induced hypoglycemia in the male rat. Neuropeptides 2017; 66: 25–35. [PubMed: 28823463]

Mandal SK, Shrestha PK, Alenazi FSH, Shakya M, Alhamami HN, Briski KP. Effects of estradiol on lactoprivic signaling of the hindbrain upon the contraregulatory hormonal response and metabolic neuropeptide synthesis in hypoglycemic female rats. Neuropeptides 2018; 70:37–46. [PubMed: 29779845]

Mathieu C, Li de la Sierra-Gallay I, Duval R, Xu X, Cocaign A, Leger T, Woffendin G Camadro JM, Etchebest C, Haouz A, Dupret JM, Rodrigues-Lima F Insights into brain glycogen metabolism: the structure of human brain glycogen phosphorylase. J. Biol. Chem 2016; 291: 18072–18083. [PubMed: 27402852]

Mizuno Y, Oomura Y. Glucose responding neurons in the nucleus tractus solitarius of the rat: in vitro study. Brain Res. 1984; 307: 109–116. [PubMed: 6147174]

Müller MS, Pedersen SE, Walls AB, Waagepetersen HS, Bak LK. Isoform-selective regulation of glycogen phosphorylase by energy deprivation and phosphorylation in astrocytes. Glia 2015; 63: 154–162. [PubMed: 25130497]

Nadeau OW, Fontes JD, Carlson GM. The regulation of glycogenolysis in the brain. J. Biol. Chem 2018; 293: 7099–7107. [PubMed: 29483194]

Oomura Y, Ono T, Ooyama H, Wayner MJ. Glucose and osmosensitive neurones of the rat hypothalamus. Nature 1969; 222: 282–284. [PubMed: 5778398]

Routh VH, Hao L, Santiago AM, Sheng Z, Zhou C. Hypothalamic glucose sensing: making ends meet. Front Syst Neurosci. 2014; 8:236. doi: 10.3389/fnsys.2014.00236. [PubMed: 25540613]

Sagar SM, Sharp FR, Swanson RA. The regional distribution of glycogen in rat brain fixed by microwave irradiation. Brain Res. 1987; 417: 172–174. [PubMed: 3304537]

Shakya M, Shrestha PK, Briski KP. Hindbrain 5'-adenosine monophosphate-activated protein kinase mediates short-term food deprivation inhibition of the gonadotropin-releasing hormone-luteinizing hormone axis: role of nitric oxide. Neuroscience 2018; 383:46–59. [PubMed: 29746990]

Shrestha PK, Tamarkar P, Ibrahim BA, Briski KP. Hindbrain medulla catecholamine cell group involvement in lactate-sensitive hypoglycemia-associated patterns of hypothalamic norepinephrine and epinephrine activity. Neuroscience 2014; 278: 20–30. [PubMed: 25084049]

Silver IA, Erecińska M. Glucose-induced intracellular ion changes in sugar-sensitive hypothalamic neurons. J. Neurophysiol 1998; 79: 1733–1745. [PubMed: 9535943]

Uddin MM, Mahmood ASMH, Ibrahim MMH, Briski KP. Sex-dimorphic estrogen receptor regulation of ventromedial hypothalamic nucleus glucoregulatory neuron adrenergic receptor expression in hypoglycemic male and female rats. Brain Res. 2019; 10 1; 1720:146311. doi: 10.1016/j.brainres.2019.146311. [PubMed: 31265816]

Yettefti K, Orsini JC, Perrin J. Characteristics of glycemia-sensitive neurons in the nucleus tractus solitarii: possible involvement in nutritional regulation. Physiol. Behav 1997; 61: 93–100. [PubMed: 8976538]

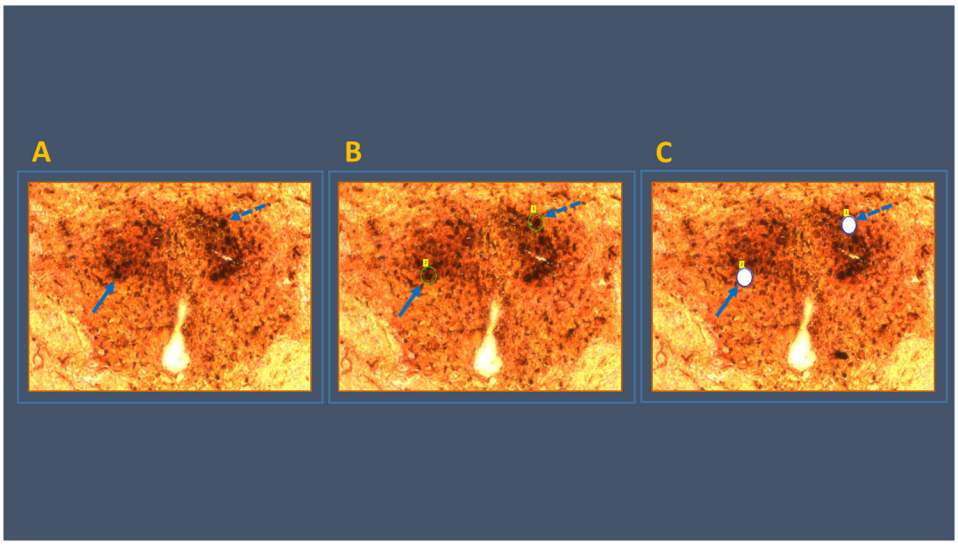

Figure 1. Laser-Catapult Microdissection of Immuno-Characterized Hindbrain Dorsal Vagal Complex A2 Noradrenergic.

A2 neurons located between 14.36 to 14.86 mm posterior to *bregma* were identified *in situ* for tyrosine hydroxylase (TH) immunoreactivity (-ir); pre-dissected TH-ir-positive neurons in Panel 1A are denoted by blue arrows. The area shown in Panel 1A was re-photographed after positioning of a continuous laser track (depicted in green) around individual TH-ir neurons [Panel 1B] and subsequent ejection of each cell by laser pulse [Panel 1C]. Note that this microdissection technique causes negligible destruction of surrounding tissue and minimal inclusion of adjacent tissue.

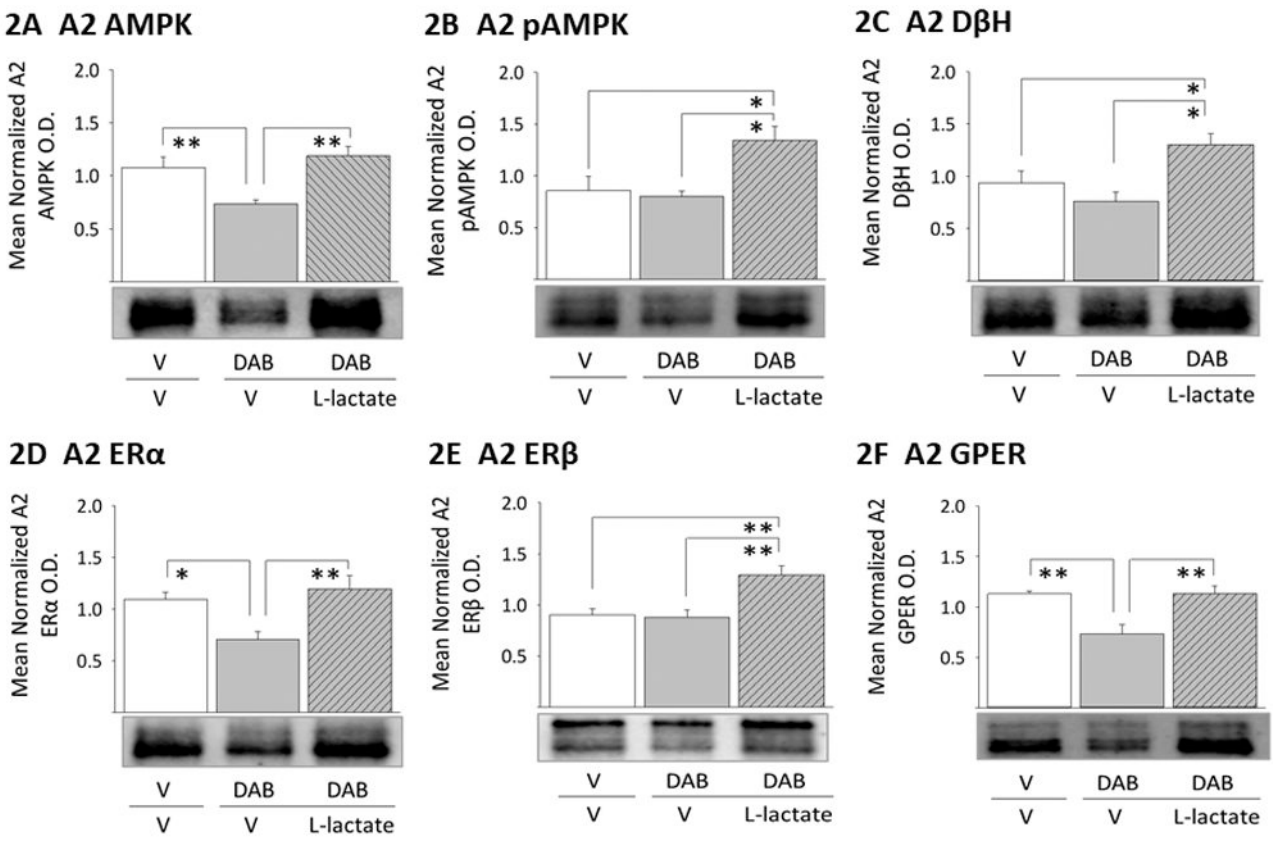

Figure 2. Effects of Caudal Fourth Ventricular (CV4) Administration of the Glycogen Phosphorylase (GP Inhibitor 1,4-Ddideoxy-1,4-Imino-d-Arabinitol (DAB) on Dorsal Vagal Complex A2 Noradrenergic Neuron Energy Gauge, Catecholamine Biosynthetic Enzyme Marker, and Estrogen Receptor (ER) Variant Protein Expression: Impact of Exogenous L-Lactate Infusion.

Groups of adult male rats were treated by intra-CV4 administration of the vehicle artificial cerebrospinal fluid (aCSF; group 1) or DAB (groups 2 and 3) into the CV4, followed by continuous infusion of aCSF (groups 1 and 2) or L-lactate (group 3) into the same ventricle. Pooled A2 cell lysates from each treatment group were probed for 5'-AMP-Activated Protein Kinase (AMPK; Panel 2A), phosphoAMPK (pAMPK; Panel 2B), dopamine-beta-hydroxylase (DβH; Panel 2C), ER-alpha (ERα; Panel 2D), ER-beta (ERβ; Panel 2E), or G protein-coupled estrogen receptor-1 (Panel 2F) protein expression. Bars depict mean normalized protein optical density (O.D.) values ± S.E.M. for aCSF/aCSF (solid white bars), DAB/aCSF, and DAB/L-lactate treatment groups. *p<0.05; **p<0.01; ***p<0.001.

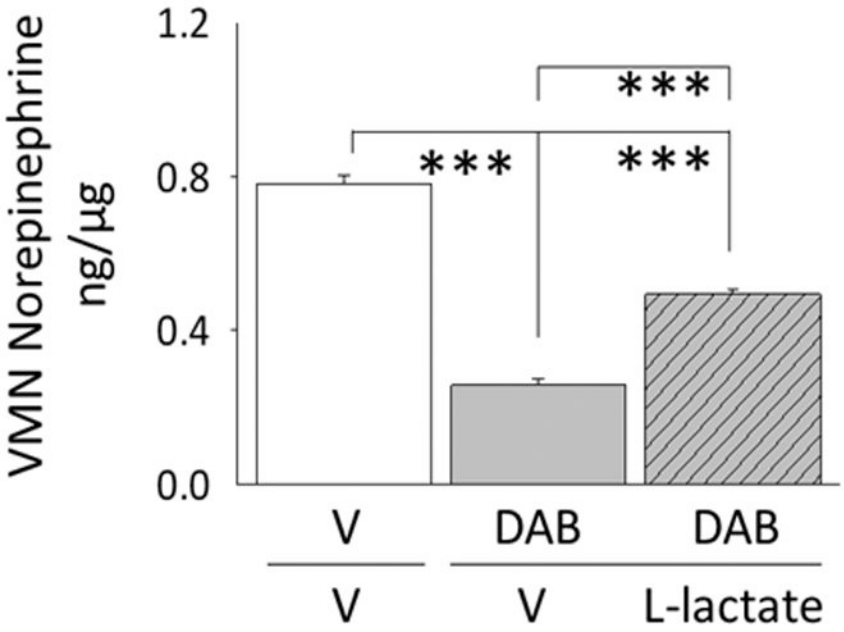

Figure 3. Impact of Pharmacological Inhibition of Hindbrain GP With or Without Exogenous Lactate Infusion on Ventromedial Hypothalamic Nucleus Norepinephrine (NE) Content.

Bars show mean VMN tissue NE levels for aCSF/aCSF (solid white bars), DAB/aCSF (solid gray bars), and DAB/L-lactate (diagonal-striped gray bars) treatment groups. *p<0.05; **p<0.01; ***p<0.001.

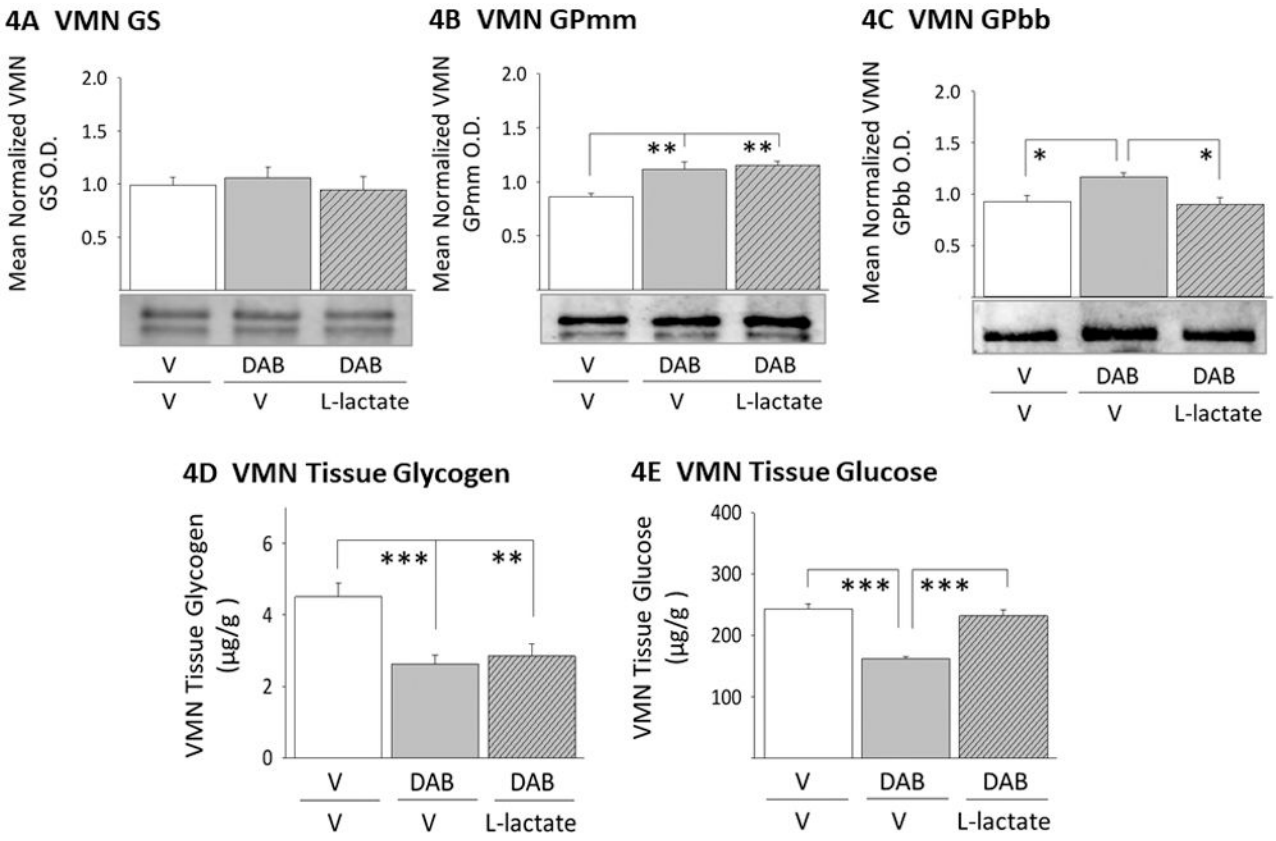

Figure 4. Regulation of VMN Glycogen Metabolic Enyzme Protein Expression and Glycogen Content by Hindbrain Glycogen Metabolic Status.

In Panels 4A-3C, bars depict mean normalized VMN glycogen synthase (GS; Panel 4A), glycogen phosphorylase-brain type (GPbb; Panel 4B), or glycogen phosphorylase GP-muscle type (GPmm; Panel 4C) protein O.D. measures ± S.E.M. for aCSF/aCSF (solid white bars), DAB/aCSF (slid gray bars), and DAB/L-lactate (diagonal-striped gray bars) treatment groups. Data in Panels 3D and 3E illustrate DAB effects with or without subsequent L-lactate infusion on mean VMN glycogen or glucose content, respectively, in the same treatment groups. *p<0.05; **p<0.01; ***p<0.001.

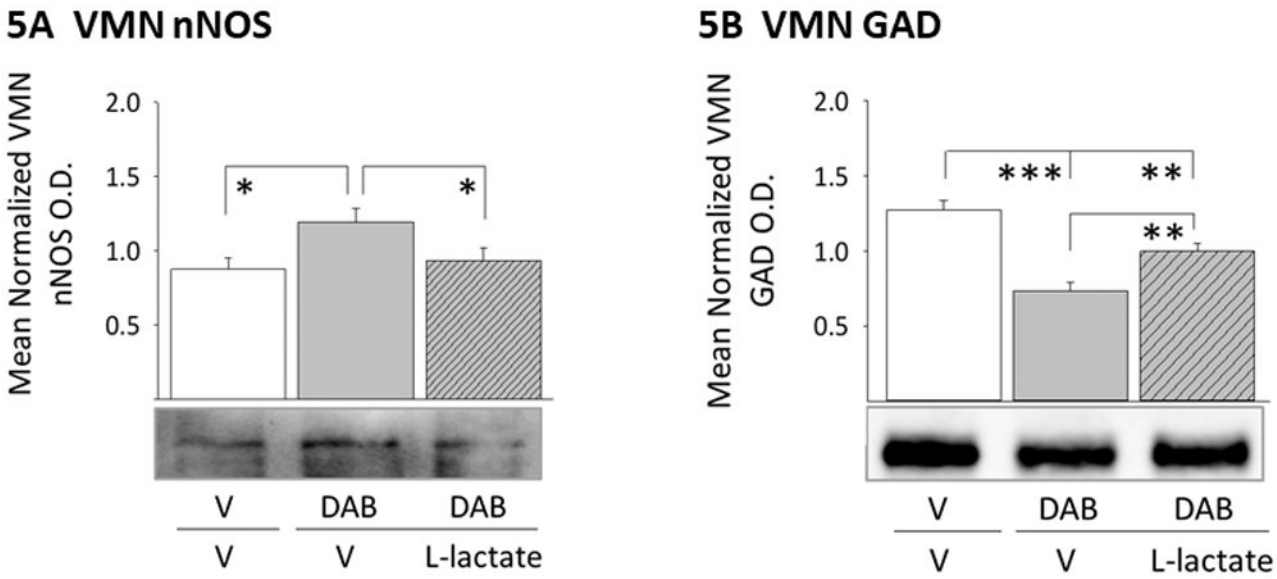

Figure 5. Effects of Hindbrain GP Inhibition on VMN Gluco-stimulatory Nitrergic and Gluco-inhibitory γ-Aminobutyric Acid Neuron Marker Protein Expression; Impact of L-Lactate Infusion.

Bars in Panels 5A and 5B depict mean normalized VMN neuronal nitric oxide synthase (nNOS) or glutamate decarboxylase 65/67 (GAD) protein O.D. measures ± S.E.M. for aCSF/aCSF (solid white bars), DAB/aCSF (solid gray bars), and DAB/L-lactate (diagonal-striped gray bars) treatment groups. *p<0.05; **p<0.01; ***p<0.001.

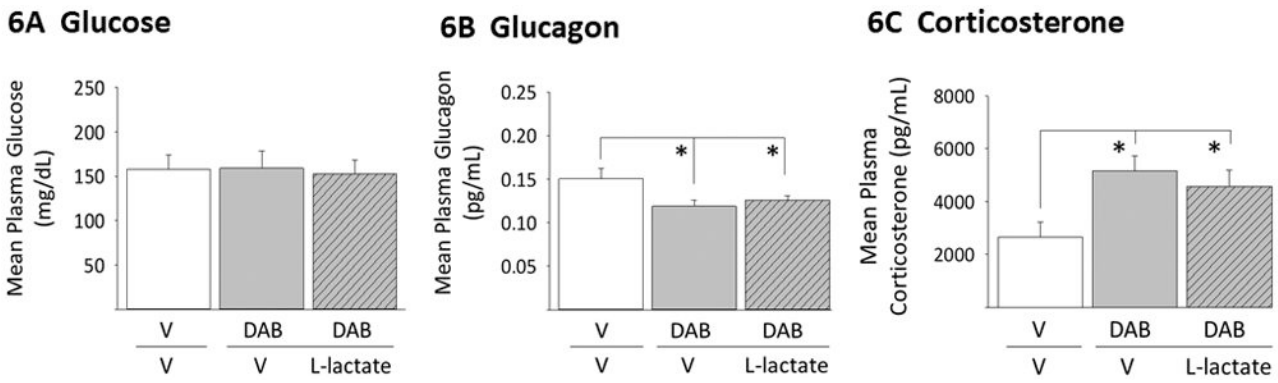

Figure 6. Effects of Caudal Fourth Ventricular DAB Administration on Circulating Glucose and Counter-Regulatory Hormone Concentrations in the Male Rat.

Data depict mean plasma glucose (Panel 6A), glucagon (Panel 6C), and corticosterone (Panel 6C) levels ± S.E.M. for aCSF/aCSF (solid white bars), DAB/aCSF (solid gray bars), and DAB/L-lactate (diagonal-striped gray bars) treatment groups. *p<0.05; **p<0.01; ***p<0.001.